# CHAPER IV

# RESULTS AND DISCUSSIONS

## 4.1 Substrate Preparation

Chromium nitride thin films were deposited on Si (100) substrates by reactive d.c. magnetron sputtering technique. Prior the growth, the substrates were ultrasonically cleaned in trichroloethylene, acetone, alcohol and de-ionized water, respectively. Then, the substrates were chemically etched by dipping 10% HF. At the end, the substrates were dried blow before introducing into vacuum chamber and pump down to vacuum.

## 4.2 $Cr_xN$ Thin Film Synthesis

In the reactive sputtering process, chromium nitride thin films were produced from a pure chromium target in a mixing of argon and nitrogen pressure. Argon is inert gas while nitrogen is reactive gas. First, argon and nitrogen gas were introduced into the vacuum chamber. Then, high voltage was applied to cathode, which was connected to the chromium target. Via the magnetron, if there was enough energy, the ionization of Ar and $N_2$ would be occurred and produce $N_2^+$ and $Ar^+$. The electric field in the system forced the ions of Ar and $N_2$ to bombard the target. When $N_2^+$ ions bombarded the target, the reaction between the ions and surface atoms of the target could be happened, as shown in Figure 4.1. Then, chromium nitride compound was formed on the target surface. This phenomenon is called "surface nitridation". At the same time, $Ar^+$ ions, which didn't react with the surface atoms, bombarded the target and created the sputtering process. Chromium nitride atoms/clusters would be sputtered from the target surface and formed chromium nitride thin film on the substrate if they had sufficiently high energy.

Apart from ejecting of the chromium nitride atoms/clusters from the target during the sputtering process, secondary electrons also emitted at the same time. These secondary electrons could be used as an advantage by the magnetron. The

secondary electrons were trapped near the target surface. This phenomenon leaded to an increasing of the ionization of gas atoms and also the ion bombardment of the target. As a result, the higher sputtering and higher deposition rate could be achieved than that in the basic sputtering.

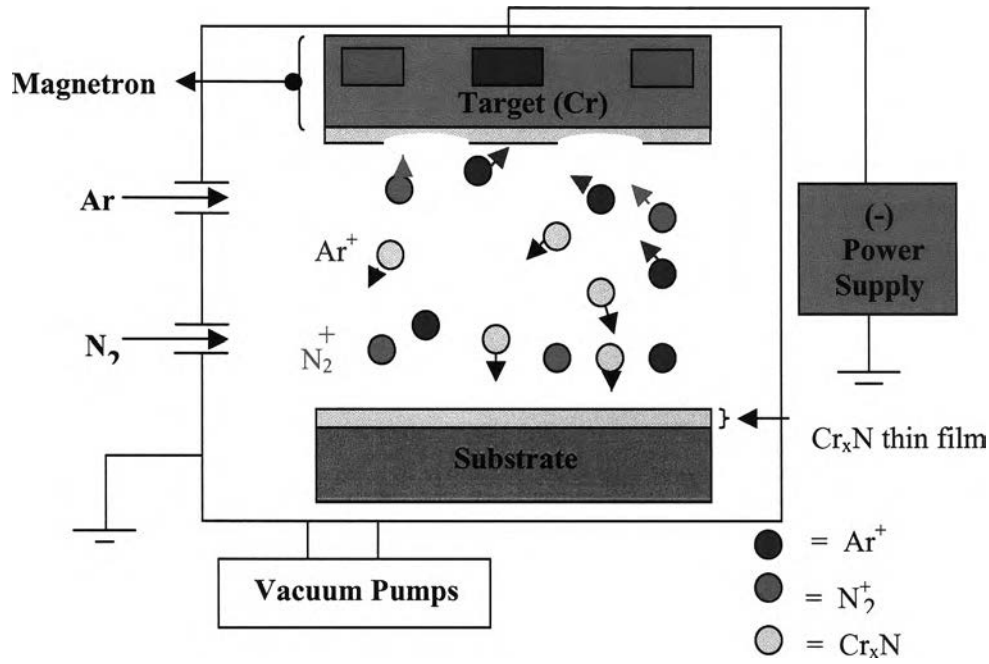


Figure 4.1: Schematic of reactive magnetron sputtering of chromium nitride thin film

## 4.3 Optimized Condition for $Cr_xN$ Thin Films

For finding the optimized condition of Ar and $N_2$ partial pressure, the partial pressure of $N_2$ was varied. The deposition parameters that used in the process are summarized in Table 4.1.

Table 4.1: Deposition parameters

| Bias voltage | 0 V |
|---|---|
| Substrate temperature | 300 °C |
| Magnetron current | 0.15 A |
| Magnetron voltage | 600 V |
| Power consumption | 90 W |
| Deposition time | 2000 s |

The $N_2$ concentration in chromium nitride thin film was analyzed by EDX. The results are shown in Figure 4.2.

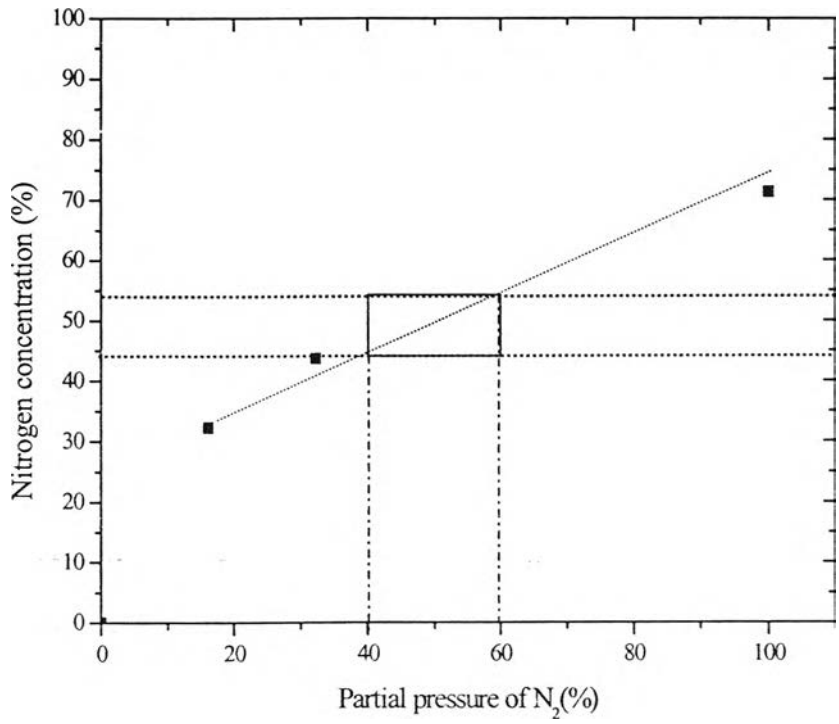


Figure 4.2: Variation of nitrogen concentration vs. $N_2$ partial pressure

From the result, nitrogen concentration increases almost linearly with a increasing of partial pressure of $N_2$ at constant substrate temperature 300 °C. The requirement composition of nitrogen in the film is in the range between 45 % and 55 %. This composition makes the film be stoichiometric. When the nitrogen

concentration is higher than 55 %, the chromium nitride film becomes over-stoichiometric. On the other hand, when the nitrogen concentration is lower than 45 %, the chromium nitride film turned to be under- stoichiometric. So, the condition of the $N_2$ partial pressure should be between 40 % and 60 % of the total pressure.

From the previous experiment, the information about the optimized partial pressure of $N_2$ that made $Cr_xN$ thin films form was obtained. In the next experiment, the substrate temperature was varied from room temperature to 250 °C. Another set of samples was made. Major deposition parameters that used in this experiment are summarized in Table 4.2.

Table 4.2: Main deposition parameters

| | |
|---|---|
| Bias voltage | 0 V |
| Growth temperature | RT – 250 °C |
| The partial pressure of $N_2$ | 50.62 % |
| The Ar flow | 6.7 sccm |
| The nitrogen flow | 8.7 sccm |
| Magnetron current | 1 A |
| Magnetron voltage | 450 V |
| Power consumption | 450 W |
| Deposition time | 1 hr |
| The distance between the target and substrate | 13 cm |

## 4.4 Structural Properties of Chromium Nitride Thin Films

The chemical composition of chromium nitride thin films as a function of substrate temperature was measured by using EDS. The results are summarized as a graph in Figure 4.3.

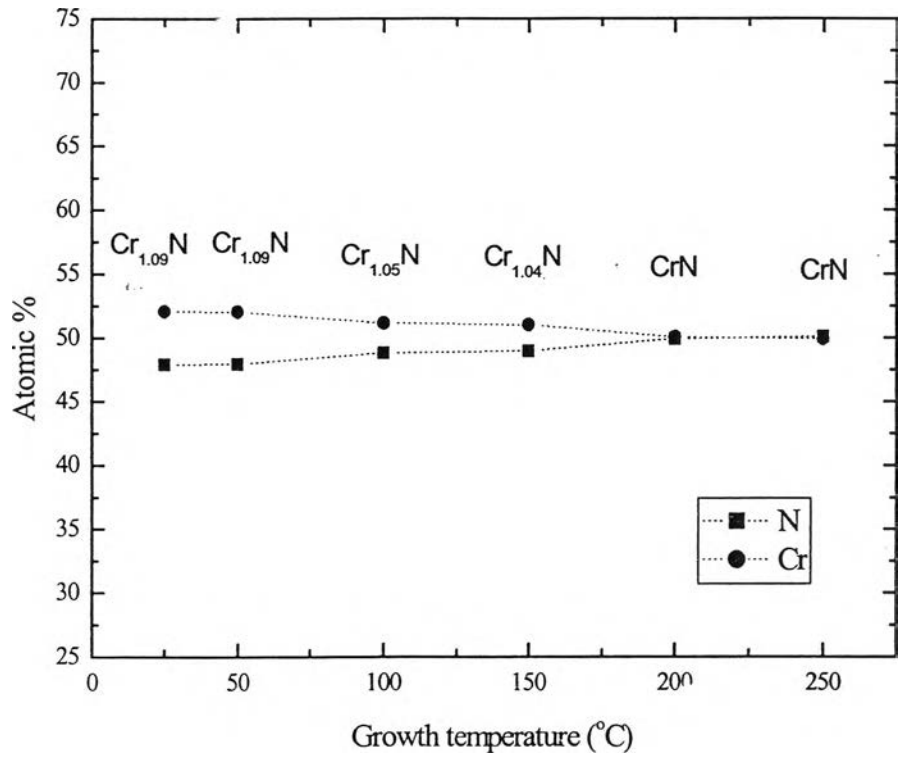


Figure 4.3: Variation of Cr/N ratio for $Cr_xN$ films with various growth temperatures

The result in Figure 4.3 shows the contents of chromium and nitrogen at different growth temperatures. All samples grown between room temperature and 250 $^0$C are stoichiometrical films. This result confirms that the nitrogen partial pressure in this process is appropriate to make stoichiometrical CrN thin films. The nitrogen content within all the films is in the acceptable range for the stoichiometric CrN material.

For the structural characterization, the XRD spectra of $Cr_xN$ thin films that deposited at different growth temperatures from room temperature to 250 $^0$C are shown in Figure 4.4.

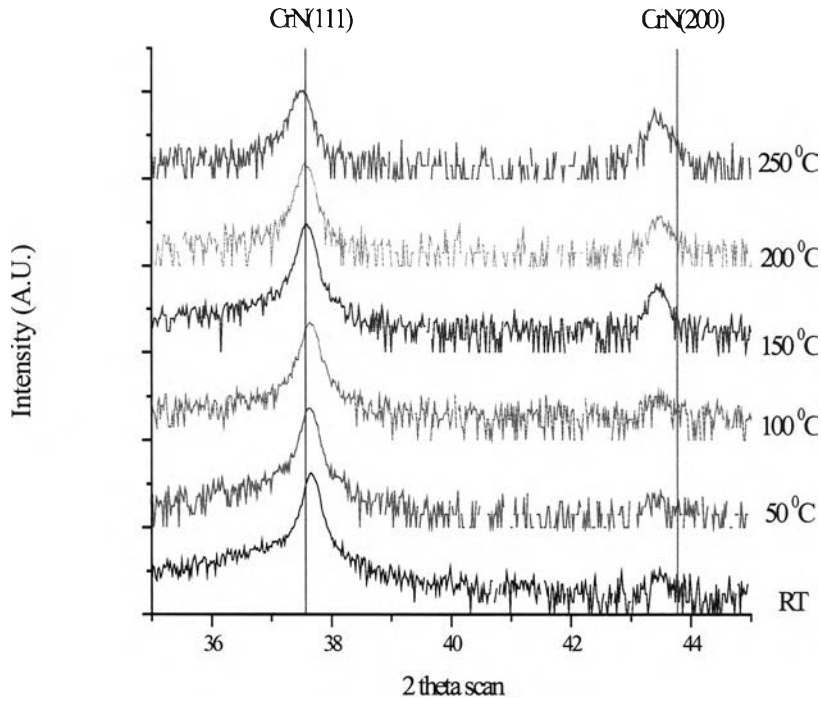


Figure 4.4: XRD patterns of six samples in different growth temperature

As seen in the figure, CrN (111) dominates at all growth temperatures; however, CrN (200) starts to develop at the growth temperature of 100 °C and tends to increase as the growth temperature increases. Figure 4.5 demonstrates the variation of texture coefficient, which is $T = \frac{I_{200}}{I_{111} + I_{200}}$ versus the growth temperature [39]. This ratio tends to increase indicating a change from (111) orientation to (200) orientation when the growth temperature increases.

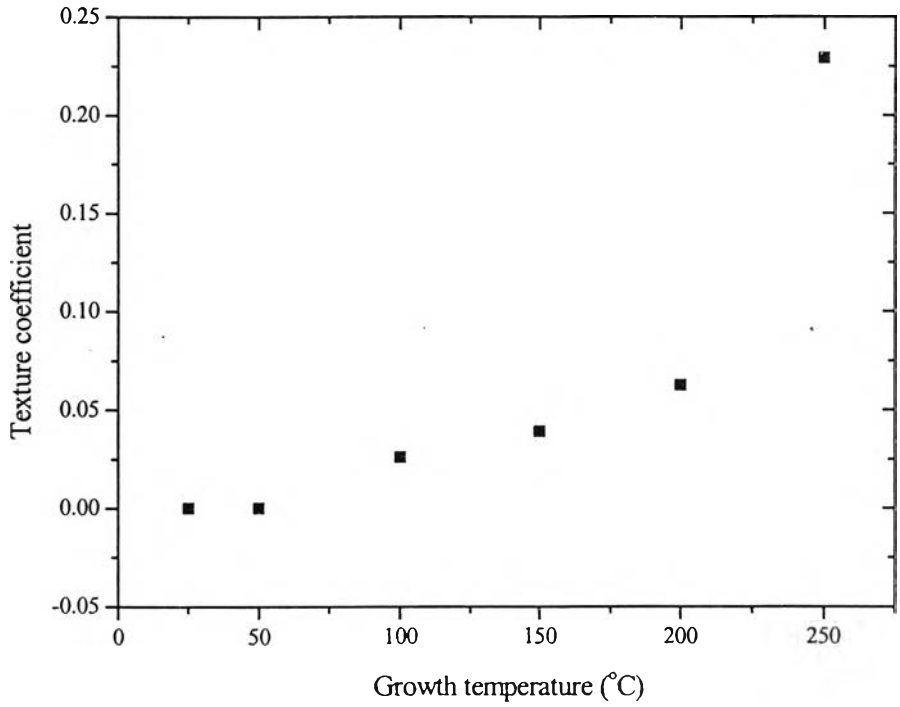


Figure 4.5: Variation of texture coefficient versus the growth temperature

The position of CrN (200) peaks shifts towards lower 2θ values in Figure 4.4. It can be explained that the diffraction angles θ decreases due to an increasing of d spacing. Consequently, the strain of CrN (200) occurs in the films. However, the position of CrN (111) peaks is close to the database information.

In this work, the $Cr_xN$ thin films grown on Si(100) substrate. The structure of Si substrate is face center cubic having the lattice constant of 5.43 Å. For discussion of the interface between the film and the substrate, the top view of Si(100), CrN(111) and CrN(200) are considered, as illustrated in Figure 4.6.

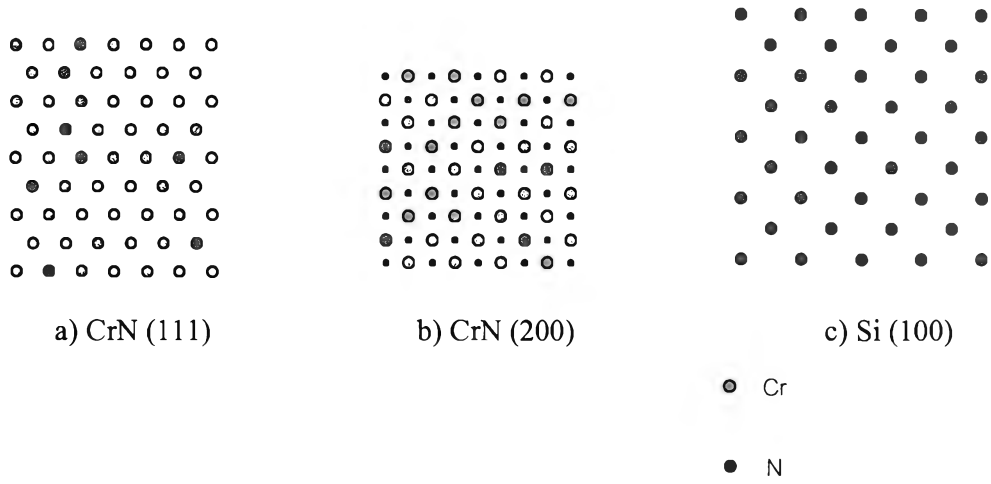


Figure 4.6: Arrangement of top atoms in CrN (111) (a), CrN (200) (b) and Si(100) plane (c)

The arrangement of Si atoms is similar to CrN (200). In case of CrN (111), the atoms are closer to each other. When $Cr_xN$ films were grown on the Si substrate, many Cr and N atoms don't react with the Si substrate atoms, the relaxation of CrN (111) and CrN (200) is occurred.

In general, for low growth temperatures, the growth of $Cr_xN$ film is controlled by the surface energy [40] resulting in the (111) preferred orientation. For higher growth temperatures, the growth of $Cr_xN$ thin films is controlled by the strain energy [28] and as the result the (200) plane is occurred. The (111) plane, which has the lowest surface energy [39], can be seen at all growth temperatures. In addition, the (200) plane is the stable surface [40] and has the lowest strain energy. As the result, the (200) plane can be occurred at the higher growth temperatures. This mechanism is called recrystallization. In this work, there is competitive growth between (111) and (200). The CrN (111) plane is preferred orientation in all growth temperatures while the CrN (200) plane is slow growth. This is due to the kinetic limitation rather than thermodynamic driving force [41]. In addition, the microstructure evolution during the film growth can be occurred due to increasing diffusion of transition metal atoms in crystalline plane. This evolution develops from the lowest surface energy to the plane with higher surface energy [42].

In addition, the full width at half maximum (FWHM) can be determined from the XRD peak by fitting the peak width with a Pseudo-Voigt function [30], as shown in Figure 4.7. This method needs single peak.

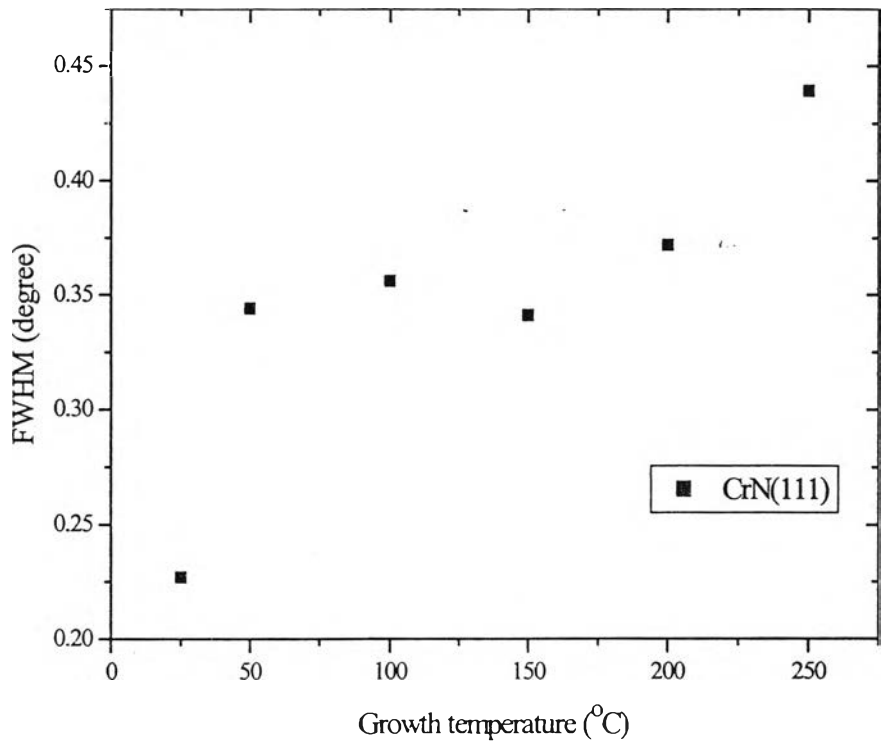


Figure 4.7: FWHM as a function of the growth temperature

The peak broadening appears because of the crystal imperfection. This imperfection is due to the mosaic structure in the film [32]. At the higher growth temperatures, the mosaic structure is increased. The FWHM of CrN (111) tends to increase as the growth temperature increases. This is due to development of the CrN (200) and a competitive growth mode between CrN (111) and CrN (200) [42]. Due to broadening peak of CrN (200), the non-uniform strain can be occurred at this plane [32].

The surface topography of $Cr_xN$ thin films was investigated by scanning tunneling microscope (STM) and atomic force microscope (AFM), as shown in micrographs of Figure 4.8 and Figure 4.9, respectively.

The results show a mixing between the large grain and small grain. According to the structure zone schematic in Figure 2.11, the melting temperature of CrN is 1773 K [43] that makes the ratio of the substrate temperature to the film melting

temperature is between 0.168 and 0.295 at the growth temperatures from room temperature up to 250 °C. The structural zone of the $Cr_xN$ thin films is mixed between the "zone 1" and "zone T". This is due to the diffusion of adatoms on the substrate is limited.

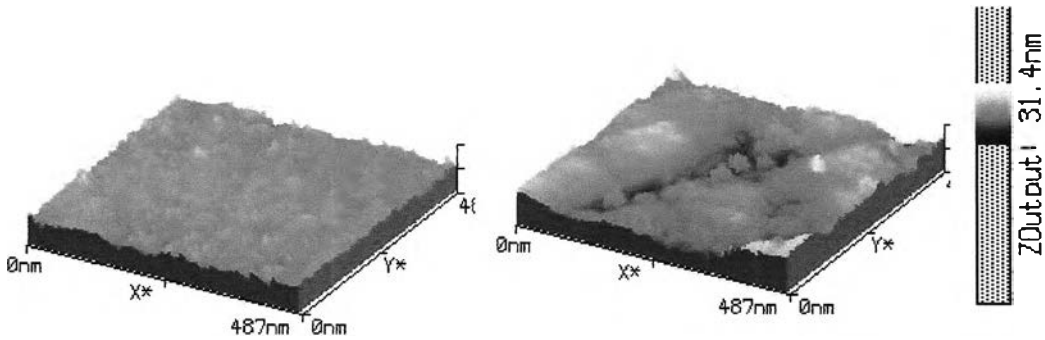


a) Room temperature b) 50 °C

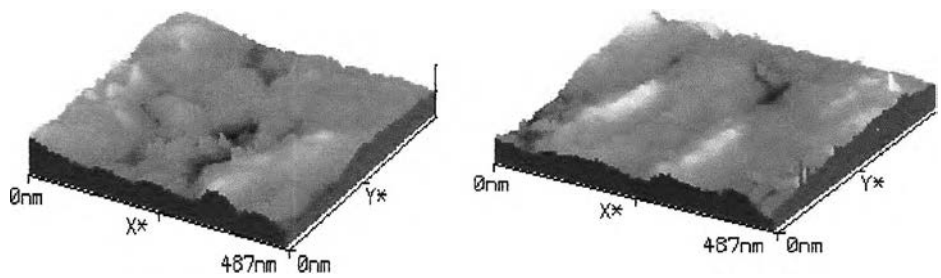


c) 100 °C d) 150 °C

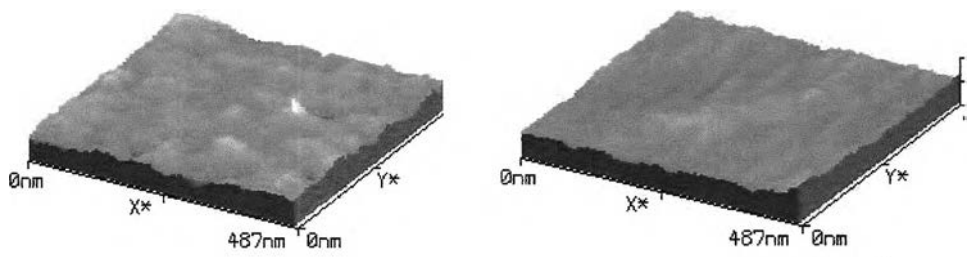


e) 200 °C f) 250 °C

Figure 4.8: STM image of $Cr_xN$ thin films on various growth temperatures

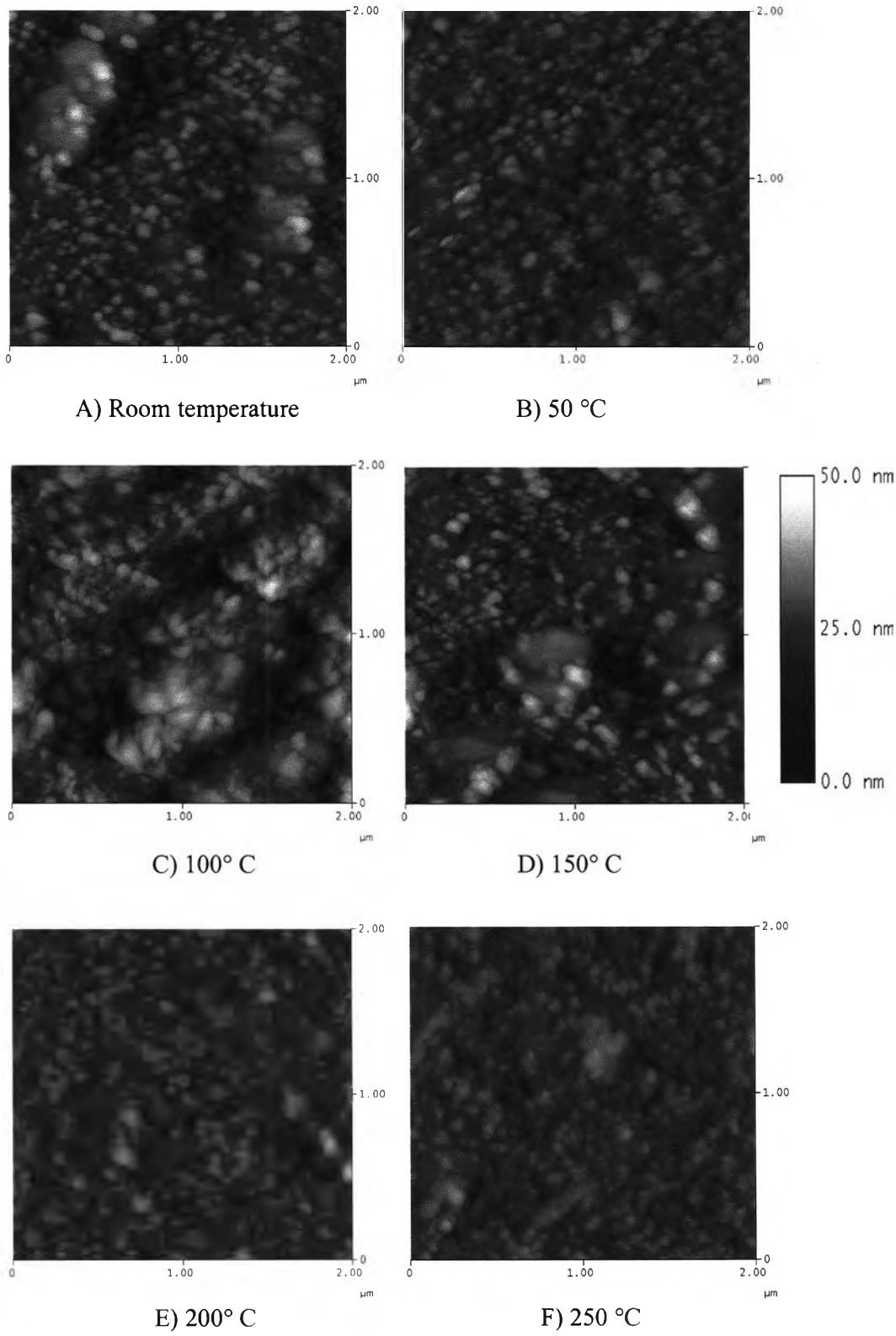


A) Room temperature B) 50 °C

C) 100° C D) 150° C

E) 200° C F) 250 °C

Figure 4.9: AFM image of $Cr_xN$ thin films on various growth temperatures

Roughness of the films can be evaluated from the AFM images, as shown in Figure 4.10.

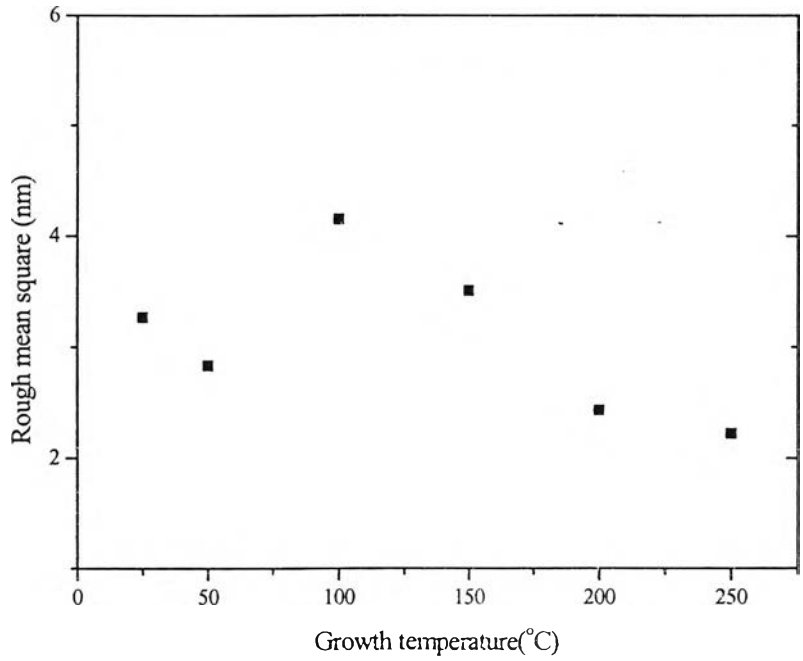


Figure 4.10: Roughness of $Cr_xN$ thin films on various growth temperatures

Figure 4.10 shows the roughness of $Cr_xN$ thin films on various growth temperatures. As the growth temperature increases, the roughness is decreased. This is due to an increasing of adatoms mobility when growth temperature increases. From the result, the roughness of $Cr_xN$ thin films, which grown at 100 ° C, is the maximum value because the competition between the CrN (200) and CrN (111) occurs.

## 4.5 Tribological Properties of Chromium Nitride Thin Films

Preliminary hardness of $Cr_xN$ thin films was measured by standard test method for film hardness by pencil test (ASTM D3363-05). A set of calibrated wood pencils for the scale of hardness is:

6B – 5B – 4B – 3B – 2B – B- HB – F – H –2H – 3H – 4H- 5H- 6H

Softer Harder

The maximum hardness scale in this method is 6H. In this method, the films were scratched or cut by wood pencil in the length of $\frac{1}{4}$ inches, as illustrated in Figure 4.11.

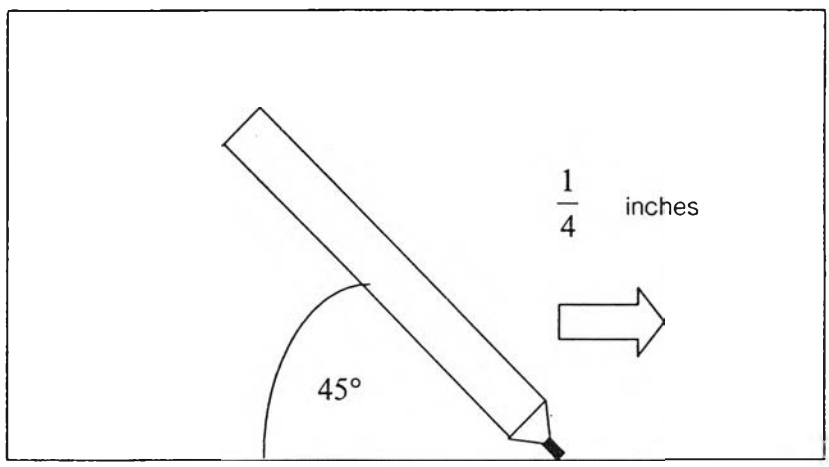


Figure 4.11: View of wood pencil with against the film at a 45° angle

These processes were done continue until the surface of the films was not be cut or scratched. In the pencil test, there are two determinations, which are *gouge hardness* and *scratch hardness*. The gouge hardness is measured from the hardest pencil that will not leave the films uncut for a stroke length of at least 3 mm. The scratch hardness is measured from the hardest pencil that will not scratch the films. The results are shown in the Table 4.3.

Table 4.3: The hardness scale on various growth temperatures

| Growth temperature (°C) | The gouge hardness | The scratch hardness |
|---|---|---|
| RT | > 6H | > 6H |
| 50 | > 6H | > 6H |
| 100 | > 6H | > 6H |
| 150 | > 6H | > 6H |
| 200 | > 6H | > 6H |
| 250 | > 6H | > 6H |

From the results, all samples have gouge hardness and scratch hardness more than 6H. This scale is the highest hardness of this method, which compares the hardness of graphite to be about 160 MPa [44]. All $Cr_xN$ thin films, which vary the growth temperature from room temperature to 250 °C, have higher hardness than graphite.

For the nanoindentation hardness test, the diamond tip is used to indent. The surface morphology of $Cr_xN$ thin films after indentation is shown in Figure 4.12.

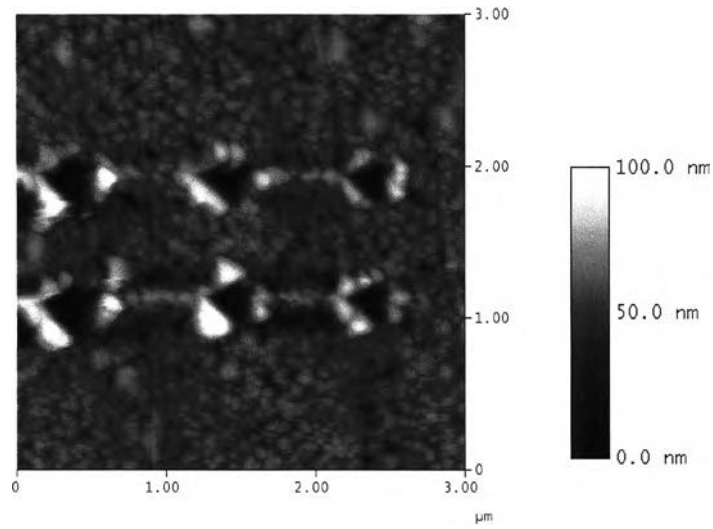


a)

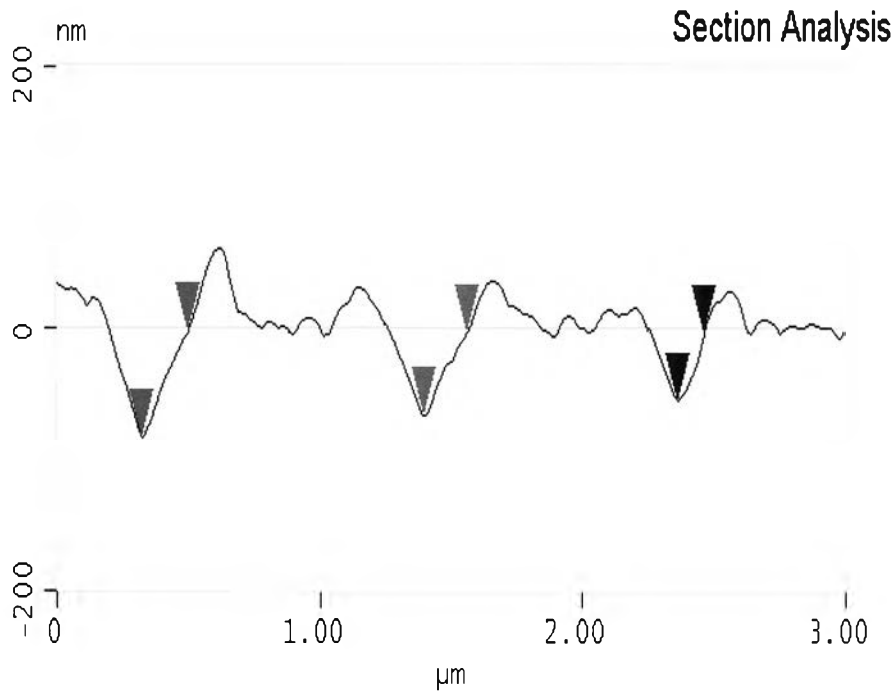


b)

Figure 4.12: Surface morphology of $Cr_xN$ thin film after indentation a) AFM morphology of six indents on $Cr_xN$ thin film and b) The cross sectional profile of three indents

Figure 4.12(a) shows the surface morphology after six indentations under 0.538 mN, 0.615 mN and 0.692 mN force load on $Cr_xN$ thin films in two rows and three columns. Each indent in the same column has the same force and the force load is varied in the row direction. The depth of $Cr_xN$ thin films after the removed tip is evaluated from the cross sectional profile as in Figure 4.12(b). The depth increases as the indentation force increases. Based on the depth, the hardness of $Cr_xN$ thin films can be calculated from equation (3.5) and (3.6). The results show in Figure 4.13.

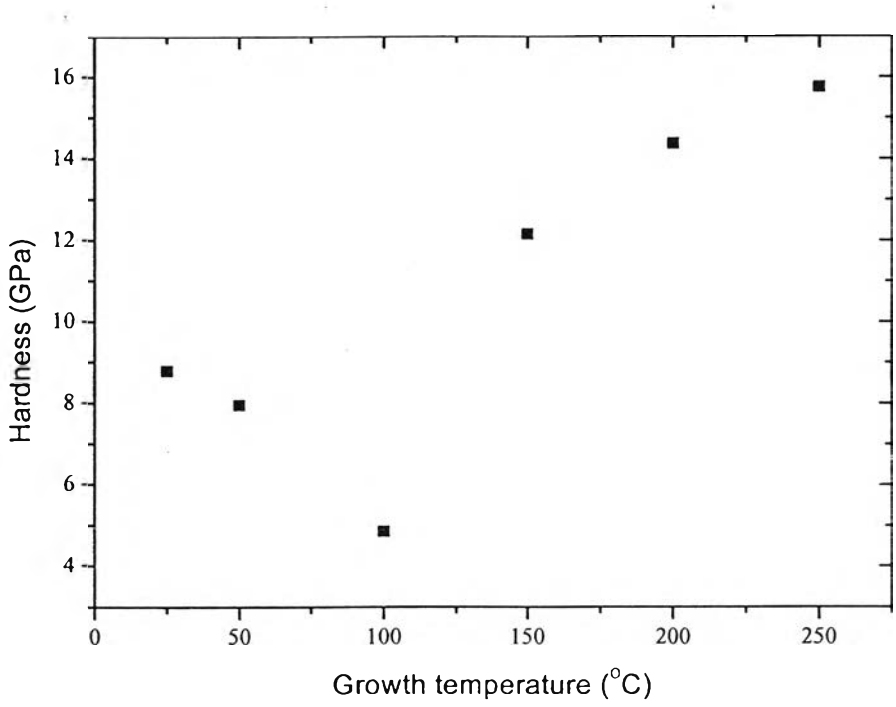


Figure 4.13: Hardness of the $Cr_xN$ films on various growth temperatures

The hardness of $Cr_xN$ films tends to increase as the growth temperature increases. This is due to the development of CrN (200) at the higher growth temperatures. The $Cr_xN$ thin film, which was grown at 250 °C, is the highest hardness with 15.74 GPa. In contrast, the $Cr_xN$ thin film, which was grown at 100 °C, is the lowest hardness with 4.85 GPa. This is due to the beginning of competition between CrN (200) and CrN (111) at growth temperature of 100 °C.

For nanoscratching test, the diamond tip is used to scratch on the surface of thin film. In this work, the scratch length is 500 nm in all samples. The surface morphology of $Cr_xN$ thin films after scratch is shown in Figure 4.14.

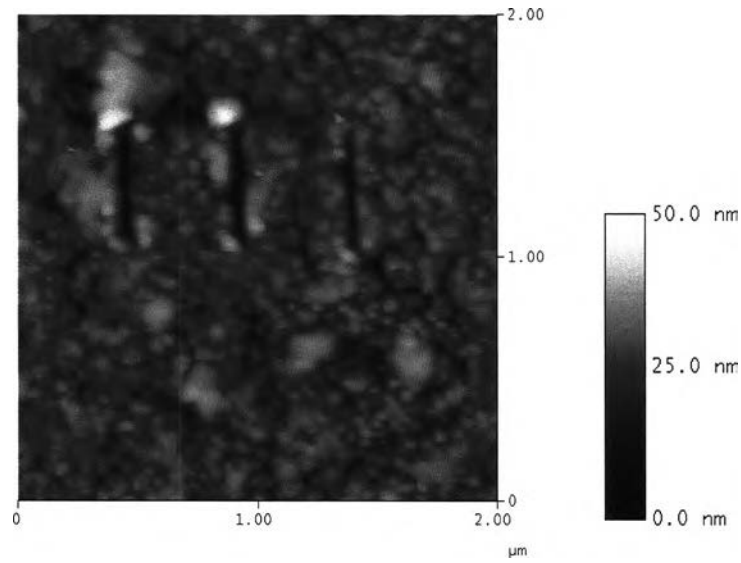


a)

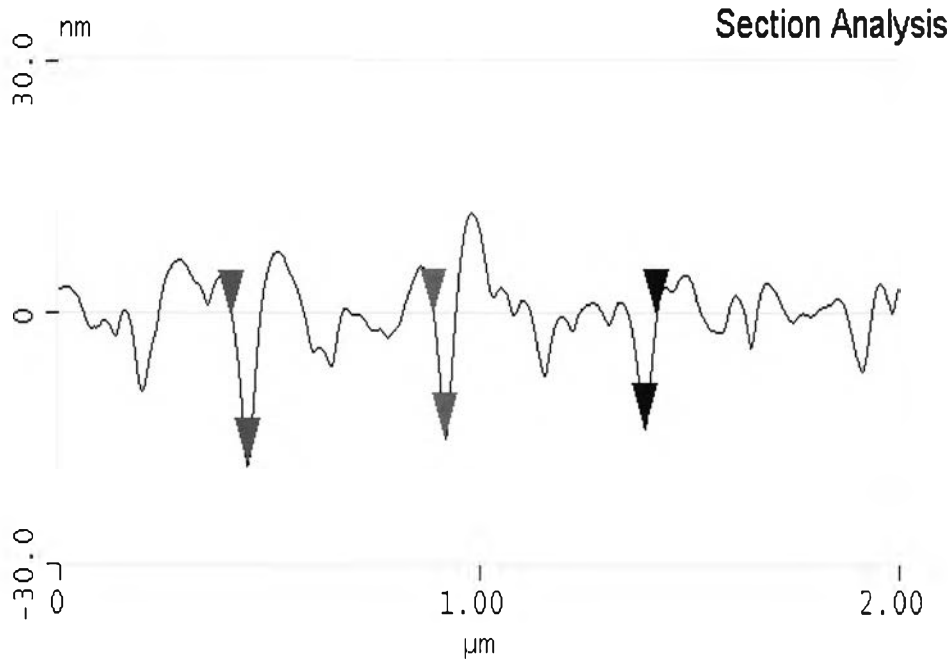


b)

Figure 4.14: Surface morphology of $Cr_xN$ thin film after scratch a) AFM morphology of three scratches on $Cr_xN$ thin film and b) The cross sectional profile of three scratches

Figure 4.14(a) shows the surface morphology of $Cr_xN$ thin film after scratch with 30.75 μN, 38.44 μN and 46.13 μN force loads. The depth can be evaluated from the cross sectional profile as in Figure 4.14(b). The residual scratch depth increases as the scratch force increases. Based on the residual scratch depth, the wear rate of $Cr_xN$ thin films can be calculated from equation (3.10). The results show in Figure 4.15.

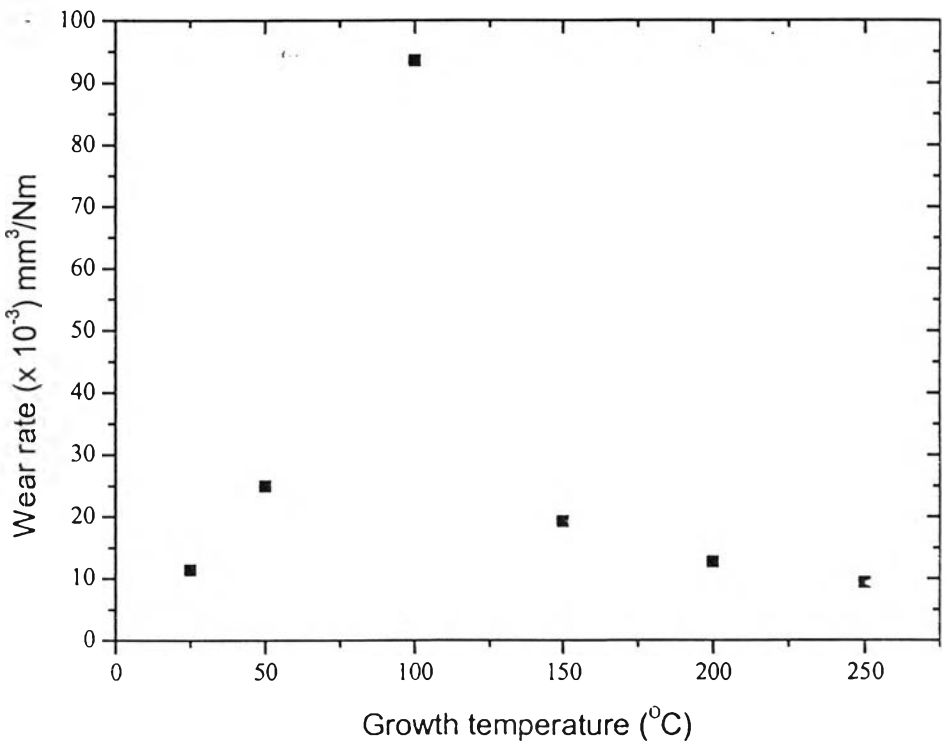


Figure 4.15: Wear rate of $Cr_xN$ thin films on various growth temperatures

The maximum wear rate value is at 93.52 x $10^{-3}$ $mm^3$/ Nm at growth temperature 100 °C. On the other hand, the minimum wear rate value is at 9.32 x $10^{-3}$ $mm^3$/ Nm at growth temperature 250 °C. From the result, it shows that the wear rate relates to the hardness value of the film. When the hardness of $Cr_xN$ thin films is high, the wear rate is low. For example, $Cr_xN$ thin film, which was grown at 250 °C, has the highest hardness and the lowest wear rate. Moreover, $Cr_xN$ thin film, which was grown at 100 °C, has the lowest hardness and the highest wear rate. In our experiment, the best growth temperature that can produce $Cr_xN$ thin film is at 250 °C with the highest wear protection.

The friction coefficient value can be calculated by using equation (3.11) and the values are shown in Figure 4.16. However, the results cannot be completed in all samples because the force curves in scratch mode of some samples cannot be achieved. This makes the friction force and the friction coefficient cannot be calculated.

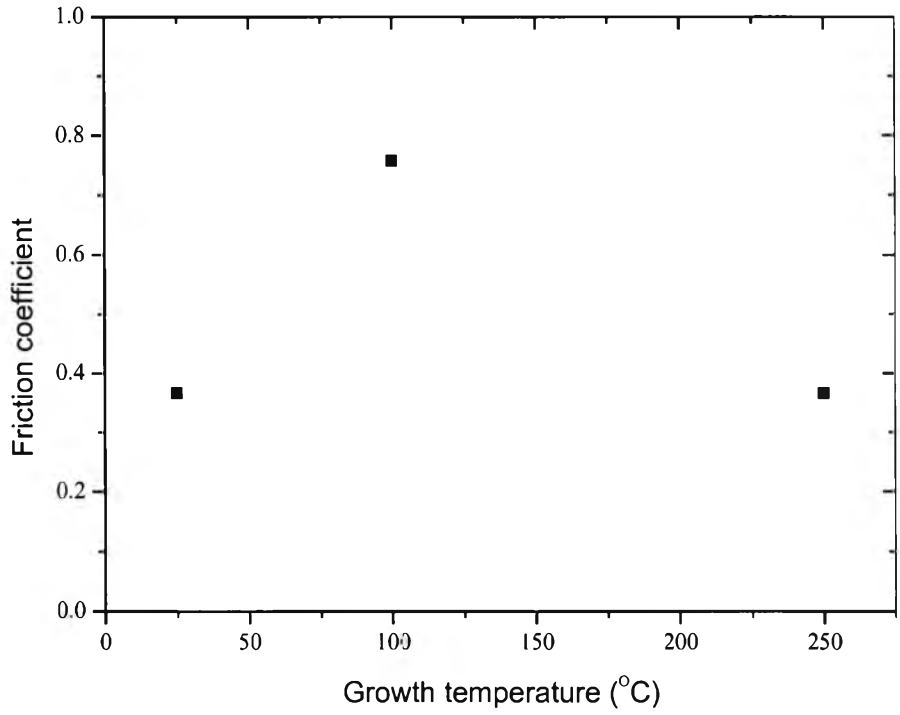


Figure 4.16: Friction coefficient as a function of the growth temperature

The friction coefficient of $Cr_xN$ thin films is 0.366, 0.757 and 0.367 at room temperature, 100 °C and 250 °C, respectively. The friction coefficient relates to the roughness of the films. For example, the CrN thin film grown at 100 °C has the highest friction coefficient and the highest roughness.

This result shows that the $Cr_xN$ thin film, which grown at 250 °C, has less roughness apart from the highest hardness and the lowest wear rate. This film is the most appropriate condition for a sensitive substrate such as plastic, aluminum and treated irons in this low growth temperature region.